Hindawi
Advances in Meteorology
Volume 2019, Article ID 7530828, 18 pages
https://doi.org/10.1155/2019/7530828

Research Article

Vertical Profile of Wind Diurnal Cycle in the Surface Boundary Layer over the Coast of Cotonou, Benin, under a Convective Atmosphere

Hagninou E. V. Donnou,[1] **Aristide B. Akpo**,[1] **Clément A. Kouchadé**,[1] **Basile B. Kounouhewa**,[1,2] **Guy H. Hounguè**,[1,2] **Gbènoukpo F. Nonfodji**,[1] **and Julien Djossou**[1]

[1]*Laboratoire de la Physique du Rayonnement, Faculté des Sciences et Techniques, Université d'Abomey-Calavi, 01 B.P. 526, Cotonou, Benin*
[2]*Centre Béninois de la Recherche Scientifique et de l'Innovation, Cotonou, Benin*

Correspondence should be addressed to Hagninou E. V. Donnou; donhelv@yahoo.fr

Received 29 October 2018; Accepted 13 February 2019; Published 1 April 2019

Academic Editor: Enrico Ferrero

The characteristics of the wind vertical profile over the coast of Cotonou during wind convective diurnal cycle were explored in this study. Wind data at 10 m above the ground and the radiosonde data in the lower 60 m of the surface boundary layer were used over the period from January 2013 to December 2016. Based on Monin–Obukhov theory, the logarithmic and power laws have allowed characterizing the wind profile. The error estimators of the Root Mean Square Error (RMSE) and the Mean Absolute Error (MAE) were, respectively, evaluated at 0.025; 0.016 (RMSE; MAE) and 0.018; 0.015. At the site of Cotonou, the atmosphere is generally unstable from 09:00 to 18:00 MST and stable for the remainder of the time. The annual mean value of the wind shear coefficient is estimated at 0.20 and that of the ground surface roughness length and friction velocity are, respectively, of 0.007 m, 0.38 $m{\cdot}s^{-1}$. A comparative study between the wind extrapolation models and the data was carried out in order to test their reliability on our study site. The result of this is that whatever the time of the year is, only the models proposed (best fitting equation) are always in good agreement with the data unlike the other models evaluated. Finally, from the models suitable for our site, the profile of wind convective diurnal cycle was obtained by extrapolation of the wind data measured at 10 m from the ground. The average wind speed during this cycle is therefore evaluated to 8.07 $m{\cdot}s^{-1}$ for August which is the windiest month and to 4.98 $m{\cdot}s^{-1}$ for the least windy month (November) at 60 m of the ground. Considering these results, we can so consider that the site of Cotonou coastal could be suitable for the installation of wind turbines.

1. Introduction

The wind resource available at hub height of a wind turbine (more than 10 m) is generally known by installing large towers or even more expensive devices such as LIDAR or SODAR to carry out the measurements. Other methods, expensive in calculation, are also used such as reanalysis data downscaling numerical models [1], statistical techniques such as autoregressive and moving average models [2], or artificial neural networks [3, 4]. These calculations methods thus increase the cost of wind projects by often making them economically not viable [5].

To cope with this difficulty, there are other simple wind speed extrapolation approaches, based on [6] and applicable only in the surface layer [7–9]. These are the power and logarithmic laws that gives a better profile of the wind speed and developed by some authors such as [6, 10–24]. However, after testing their reliability on other sites, the authors of [25–27] have reached inconclusive results. To predict the average wind speed accurately at different heights and thus the expected wind energy output, increasing knowledge on wind shear models to strengthen their reliability appears a crucial issue for investors in the wind energy field [5]. The use of these laws (power and logarithmic) requires the

knowledge of the wind shear parameters such as the roughness length of ground, the coefficient of wind friction, and the friction velocity, which are specific to each site. There is no fast, reliable, universal model to better estimate the wind speed at high altitude irrespective of the site. One of the preferable solutions that will be the subject of this study is therefore to establish a specific model for each site considered from the data, as proposed earlier by Poje and Cividini [26].

In our study area, wind data at hub height of a wind turbine is not available except the radiosonde data that are recorded once a day at 10:30 MST by the Agency for Air Navigation Safety in Africa and Madagascar (ASECNA). These data unfortunately do not cover at least the diurnal cycle of the day. The previous work done on the evaluation of the wind resource by the authors of [28–30] was therefore limited to the altitude of 10 m where the data are measured every 10 minutes and averaged every 01 h. To solve this problem of lack of wind data concerning the site of Cotonou at an altitude higher than 10 m, the radiosonde data have been exploited to evaluate and validate the two techniques of wind speed extrapolation (power and logarithmic law). Then the models parameters were determined, and a comparative study between the models available in the literature and the data was performed. The most suitable model for the site was then used to regenerate by extrapolation of the vertical profile of wind convective diurnal cycle from the data measured at 10 m from the ground. In this study, we were not interested at the nocturnal cycle of the wind due to the lack of radiosonde data during this cycle. The atmosphere slice chosen for this study (lower 60 m of the surface boundary layer) is quite reasonable for a developing country like ours, which is still in the early stages of wind energy experimentation.

2. Materials and Methods

2.1. Presentation of the Study Area and the Used Data. Radiosonde, wind speed, and ambient air temperature measurements were taken at the meteorological station of the Agency for Air Navigation Safety in Africa and Madagascar (ASECNA/National Agency of Benin Meteorology) located at Cotonou Airport in southern Benin. This region whose latitude ranges from 6°10′ N to 6°40′ N and its longitude from 1°40′ E and 2°45′ E is bounded by the crystalline peneplain in Middle Benin in the north, the Atlantic Ocean in the south, Nigeria in the east, and Togo in the West. It is part of the coastal sedimentary basin. Its climate is a subequatorial-type climate with two dry seasons and two rainy seasons [31]. By virtue of its location in the intertropical zone, Benin has a warm and humid climate. Temperatures are constantly high, with an average of 25°C for the whole country. In March are recorded the highest temperatures and in August the lowest ones [32]. Temperature variability is higher in the north of the country than that in the coastal regions. The annual thermal variations are in the region of 5 to 6°C in the coastal zone [32]. Figure 1 gives an overview of the study area.

The radiosonde data recorded and provided by the ASECNA meteorological station located at 6°21′N and 1°40′E during the period from January 2013 to December 2016 were used in this study. The series of radiosondage data used were composed of wind speeds and temperature in the lowest 60 m in the surface boundary layer (10 to 60 m above ground level in steps of 5). The radiosonde observation was carried out once a day at 10:30 MST. The wind speed data used during the same measurement period was recorded every 10 minutes and averaged every 1 hour. These data were measured from a cup anemometer placed on a mast at 10 m from the ground. The ambient temperature was also measured in the site every 1 hour. In Figure 2 is presented the equipment for measuring wind data at altitude and on the surface.

2.2. Methods

2.2.1. Method of Wind Speed Vertical Extrapolation. According to the studies [13, 33, 34], the surface roughness and the different atmospheric stability conditions have a great influence on the vertical profile of winds and must be taken into account in the estimation of the wind at altitude. The two methods of wind speed extrapolation taking into account both of these parameters and used by [17, 18, 24, 35] are in the first place of the log-linear law which is a similarity model function and secondly the power law. These two laws (log-linear law and power law) have been therefore evaluated in order to choose the best which can suitably reproduce the vertical profile of wind on our study site. They are presented in Sections 2.2.1.1 and 2.2.1.2.

(1) Log-Linear Law. The log-linear law is a function of the friction velocity, the roughness length, and the Obukhov length. According to the studies of Monin and Obukhov [6], it is defined by the following expression:

$$V_{\mathrm{h}} = \left(\frac{u_*}{\kappa}\right)\left[\ln\left(\frac{Z_{\mathrm{h}}}{Z_0}\right) - \Psi_{\mathrm{m}}\left(\frac{Z_{\mathrm{h}}}{L}\right)\right], \tag{1}$$

where L is the Obukhov length, Z_0 the roughness length, u_* the friction velocity in $\mathrm{m{\cdot}s^{-1}}$, $\Psi_{\mathrm{m}}(Z_{\mathrm{h}}/L)$ is the stability correction function, and κ the von Karman constant supposed to be equal to 0.4 and Z_{h} the height. According to the studies of Paulson [36, 37] reported by Businger [35], we have the following equation for an unstable atmospheric condition $((Z_{\mathrm{h}}/L) < 0)$:

$$\Psi_{\mathrm{m}}\left(\frac{Z_{\mathrm{h}}}{L}\right) = 2\ln\left(\frac{1+x}{2}\right) + \ln\left(\frac{1+x^2}{2}\right) - 2\tan^{-1}(x) + \frac{\pi}{2}, \tag{2}$$

where

$$x = \left(1 - 15\frac{Z}{L}\right)^{1/4}. \tag{3}$$

Two methods were exploited to determine the Obukhov length which characterizes the state of the surface layer stability. The first was based on the expression from the studies by Monin and Obukhov [6]:

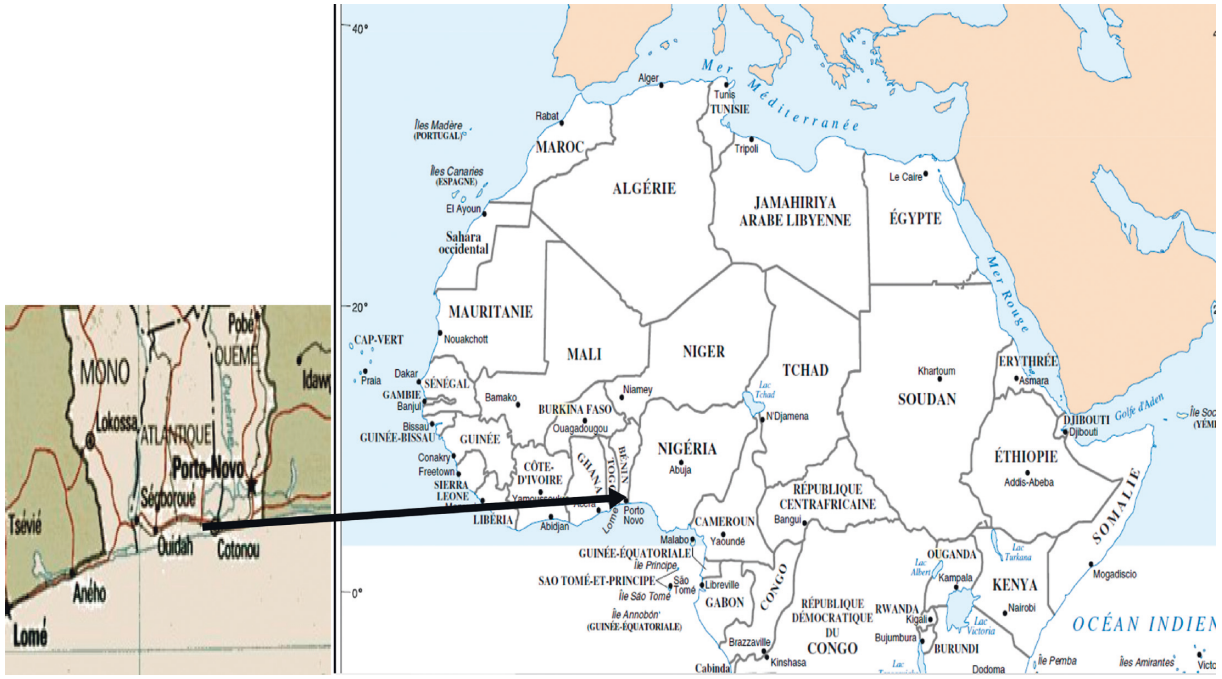

FIGURE 1: Geographical situation of the coastal zone of Benin. Location on the map of Africa [30].

$$L = -\frac{u_*^3 T_0}{\kappa g \overline{w'T'}}, \tag{4}$$

where $\overline{w'T'}$ which represents the heat flux density also refers to the covariance of the vertical wind component and the ambient air temperature T ($\overline{w'T'} = \mathrm{cov}(w,T)$), w is the vertical component of wind at 10 m of the ground, g is the gravity, κ is the von Karman constant, and T_0 is the mean temperature. $\mathrm{Cov}(w,T)$ was calculated from the Cauchy–Schwarz inequality which is based on the covariance mathematical properties. So we have

$$[\mathrm{cov}(w,T)]^2 \le \sigma^2(w)\sigma^2(T), \tag{5}$$

where $\sigma^2(T)$ is the variance of air temperature and $\sigma^2(w)$ the variance of vertical wind component.

According to [38], the vertical standard deviation σ_w can be well estimated from the parameter σ_U describing the horizontal standard deviation of wind. The best estimator is given by

$$\sigma_w = 0.45\sigma_U, \tag{6}$$

where U is the horizontal wind speed recorded by cup anemometer at 10 m of ground. The second way is based on the gradient method. According to the studies of Lange et al. [39], reported by Kasbadji [13], L was determined in terms of the Richardson number (R_i). It was estimated using the wind speed gradient and air temperature, between two different altitudes based. Thus, according to the studies of [40] reported by [19],

$$L = \begin{cases} \left(\dfrac{Z'}{10R_i}\right), & R_i < 0, \\ \dfrac{Z'(1-5R_i)}{10R_i}, & 0 \le R_i \le 0.2, \end{cases} \tag{7}$$

where

$$Z' = \frac{Z_h - Z_1}{\ln(Z_1 Z_h)}, \tag{8}$$

and Z_1 is the altitude of 10 m. $R_i = 0.25$ is the limiting value for the transition from turbulent to laminar flow. The Richardson number is provided by [20]:

$$R_i = \frac{g}{T}\frac{((\Delta T/\Delta Z) + \Gamma)}{(\Delta V/\Delta Z)^2}, \tag{9}$$

where T is the air temperature 10 m above the ground, ΔT is the temperature variation between two levels, ΔV is the variation in wind speed between two levels, Γ is the dry adiabatic temperature lapse rate, and $\Delta T/\Delta Z$ is the gradient of the air temperature according to the altitude. This latter expression of L is a function of parameters more accessible by radiosonde measurements. The results obtained by equation (4) during the diurnal cycle were used to confirm the method by radiosonde data and characterize the daily cycle. Table 1 presents the different atmospheric stability classes according to the Obukhov length.

Starting from the Monin–Obukhov theory developed in equation (1), the roughness length was determined according to the different classes of atmosphere stability knowing the vertical profile of the winds. Indeed by changing the variable, we then have

$$\begin{aligned} A &= \frac{u_*}{\kappa}, \\ B &= -A\left[\ln(Z_0) + \Psi_m\left(\frac{Z_h}{L}\right)\right]. \end{aligned} \tag{10}$$

(a) (b) (c) (d)

Figure 2: Material for measuring wind parameters. (a) Radiosonde data station and ground check. (b) The release of the probe and the balloon. (c) Cup anemometer and weather vane located on a mast of 10 m. (d) Experimentation site over the coast of Cotonou, Benin.

Table 1: Atmospheric stability classes according to the Obukhov length [41].

Stability class	Obukhov length (m)
Very stable	$0 < L < 200$
Stable	$200 < L < 1000$
Neutral	$\|L\| > 1000$
Unstable	$-200 < L < 0$
Very unstable	$-1000 < L < -200$

The form of equation (1) then becomes

$$V_h = A \ln(Z_h) + B. \tag{11}$$

Adjusting the logarithmic regression, the parameters A and B were determined. The friction velocity which represents the intensity of the turbulent air masses movement on the ground surface due to the asperities present is given by

$$u_* = A\kappa. \tag{12}$$

And the roughness length Z_0 which represents the aerodynamic effects of the topographic elements in the surface layer is determined by

$$Z_0 = \exp\left[-\left(\frac{B}{A} + \Psi_m\left(\frac{Z_h}{L}\right)\right)\right]. \tag{13}$$

(2) Power Law. The information required by the log-linear law is not always available [35], and such a method is not always easy to use for general engineering studies [42]. This is why in the studies conducted by [10], the authors preferred likening the increase in the wind speed along with the height of the surface layer to a power law. This law was proposed by [43] and reported by [14, 44–46]

$$\frac{V_h}{V_1} = \left(\frac{Z_h}{Z_1}\right)^{\alpha}, \tag{14}$$

where V_1 is the wind speed at 10 m. This law depends only on a single parameter α which is the friction or Hellman exponent, also known as wind shear coefficient. Its value depends on several factors like the atmospheric stability, ground characteristics such as topography and the roughness Z_0 [7, 47] and gives information about the variations in wind intensity according to altitude. Considering the properties of logarithms, equation (14) becomes

$$\ln\left(\frac{V_h}{V_1}\right) = \alpha \ln\left(\frac{Z_h}{Z_1}\right). \tag{15}$$

Based on equation (15), the coefficient α can be determined through the equation below:

$$\alpha = \frac{\ln(V_h) - \ln(V_1)}{\ln(Z_h) - \ln(Z_1)}. \tag{16}$$

From the studies of [36] and for an unstable atmosphere, α can be also computed by

$$\alpha = \frac{(1 - 16(Z/L))^{-(1/4)}}{\ln((\eta - 1)(\eta_0 + 1)/(\eta + 1)(\eta_0 - 1)) + 2\mathrm{Arctan}(\eta) - 2\mathrm{Arctan}(\eta_0)}, \tag{17}$$

where

$$\eta = \left(1 - 16\frac{Z}{L}\right)^{1/4}, \qquad \eta_0 = \left(1 - 16\frac{Z_0}{L}\right)^{1/4}. \tag{18}$$

These two laws (log-linear and power law) are function of the parameter α in the power law (equation (14)) and the parameters A, B included in the linear-log law (equation (11)). To evaluate their performance on our study site, we have determined the monthly and annual fitting equations of the data based on these laws. The parameters α, A, and B have therefore been obtained from these adjustments. The parameter α has been determined from the equation (16) and A, B by a logarithmic regression from equation (11). Replacing in both the previous laws the values of these calculated parameters, we obtain these fitting equations which are specific of our study area. From the statistical tests presented in Section 2.2.2, the best adjustment equations have been selected.

2.2.2. Model Validation Test. The Root Mean Square Error (RMSE) measures the average magnitude of the errors committed by the prediction. It is one of the most used indicators. For each date of prediction, the RMSEs related to wind speed predictions were calculated over the entire study period using the formula below, like many authors such as [48, 49]:

$$\mathrm{RMSE} = \sqrt{\frac{1}{N}\sum_{i=1}^{n}(p_i - f_i)^2}, \tag{19}$$

where p_i represents observations, f_i the different estimates or predictions, and N the total number of wind speed observations. The smaller its value is, the closer it is to zero and the better the model is [48]. Another test was used and considered as a little more reliable because less affected by the most important prediction errors is the Mean Absolute Error (MAE) used in the studies of [34, 50]:

$$\mathrm{MAE} = \frac{1}{N}\sum_{i=1}^{n}|(p_i - f_i)|. \tag{20}$$

3. Results and Discussions

The results obtained with regards to the characteristics of winds in the surface boundary layer of the study area are as follows.

3.1. Vertical Profile of the Wind Speed and Temperature Air. Figure 3 shows the vertical profiles of daily wind speed and ambient air temperature at a monthly scale from raw measurements of the radiosonde data.

The analysis of Figure 3(a) indicates that the profile is almost mixed up for August and July which are the windiest months in the year. The average wind speeds are, respectively, equal to 7.9 m·s^{-1} and 7.85 m·s^{-1} 60 m above the ground. Considering the months of November and December which are the least windy months, the average wind speeds are, respectively, estimated at 5.8 m·s^{-1} and 5.65 m·s^{-1} at 60 m above the ground. This variation of the wind profile can be explained by the position of the intertropical front (ITF) in the study area during the year. Indeed, the northward latitudinal migration of the ITF in the lower atmosphere, which marks the arrival of the monsoon, abruptly takes place in late June, from a nearly stationary position at 5°N in May-June to another stable position at 10°N in July-August [51]. The latter, which is intense in the study area, increases the local breezes over the continent and more precisely over the study site. The result of this is that the wind speed increases during this period. During the November-December period, the ITF begins moving southward. The northeastern trade winds (less intense in the study area) dominate the monsoon by their presence. As a result, there is a decrease in wind intensity during this period.

Figure 3(b) shows the daily vertical profile of the ambient temperature at monthly scale. The months of February, March, and April are the hottest months of the year with temperatures respectively estimated at 29.97°C, 29.88°C, and

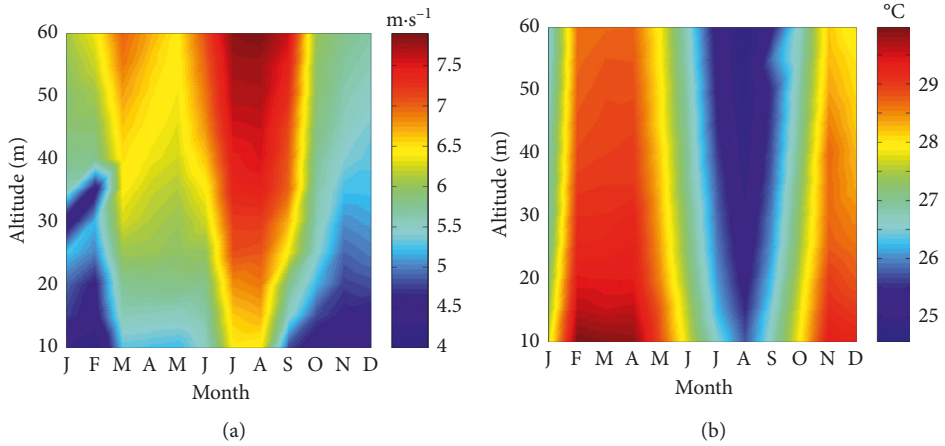

Figure 3: Vertical profile of two meteorological magnitudes. (a) Daily vertical profile of wind speed at a monthly scale and (b) daily vertical profile of the ambient temperature at a monthly scale (2013–2016).

29.85°C at 10 m above the ground and 28.62°C, 28.69°C, 28.7°C at 60 m. August is the least hot month with an estimated temperature of 25.74°C at 10 m above the ground and 24.57°C at 60 m. Figure 4 indicates the vertical profile of wind with the error bars upon the data. These error bars are computed over a period of 4 years and represent the standard deviation of measurements at each altitude from 10 to 60 m.

In Figure 4, we note after analysis that the errors made on the wind speed measurements from the radiosonde data vary from 0.73 to 0.87 m·s^{-1}. The lowest measurement error is recorded at 10 m from the ground and the highest at 35 m. These obtained values indicate thus a small proportion of error margin of wind speed measurement in the lowest 60 m in the surface boundary layer on our study site. Figure 5 shows the fitting curves of the vertical profile of wind speed for a typical day at monthly scale from the power and logarithmic law. The values of the parameters A and B obtained after the monthly adjustment are presented in Table 2.

The adjustment coefficients (α, A, B) obtained and which are function of wind shear parameters differ from one month to other and show that the vertical profile of wind does not present the same variations in function of altitude during the year. The values of parameter α are represented in Figure 6(a). The monthly fitting equations of the wind profiles are also specified in Figure 5.

The analysis of Figure 5 shows that the vertical profile of the wind speed adjustment by the power law and the logarithmic law corresponds to the measurements whatever the time of the year is. The values of the RMSE and MAE coefficients are obtained and summarized in Table 3 are low and very close. These low values therefore lead us to validate these different fitting equations based on the power law model and logarithmic law as the models of wind speed extrapolation at the site of Cotonou. These two laws can therefore be used to model the vertical wind speed profile at our study site as mentioned by the studies of [52, 53]. We also note a significant variation in the wind speed near the ground, due to the effect of the roughness and obstacles encountered on the ground, which diminishes with the altitude.

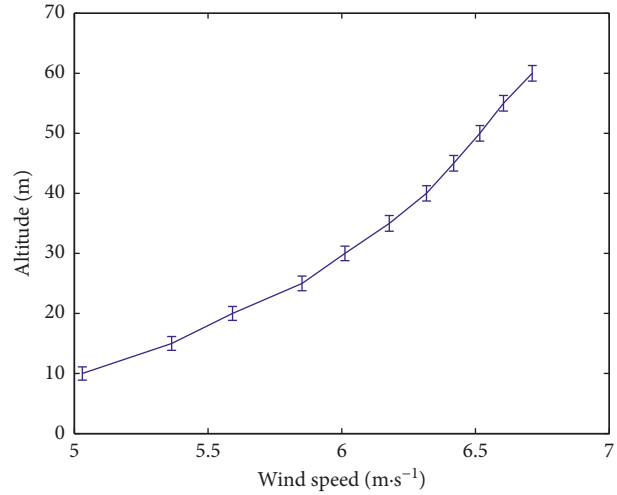

Figure 4: Vertical profile of wind with error bars recorded on a period of 4 years. The error bars represent the standard deviation of measurements for a sample of 1440 data for each altitude level.

Figure 7 shows the annual fit curve of the wind vertical profile by applying both laws and the fitting equations. The average annual speed at 10 m above the ground using the data is 5.03 ± 0.73 m·s^{-1} and is 6.71 ± 0.86 m·s^{-1} at 60 m. The estimation (RMSE; MAE) errors between these two laws and the data are, respectively, equal to 0.018; 0.015 and 0.025; 0.016 for power and logarithmic laws. These low values do indicate that these two laws are also very suitable for the estimation of the annual daily wind vertical profile at the study site.

3.2. Model Parameters. Figure 6 shows the monthly average variations in the wind shear parameters. These are the wind shear coefficient, the surface roughness length, Obukhov length, and the wind friction speed.

In Figures 6(a), 6(b), and 6(d), the average wind shear coefficient, the average surface roughness length, and friction velocity present in general the same seasonal variations. These variations clearly show that these three parameters are

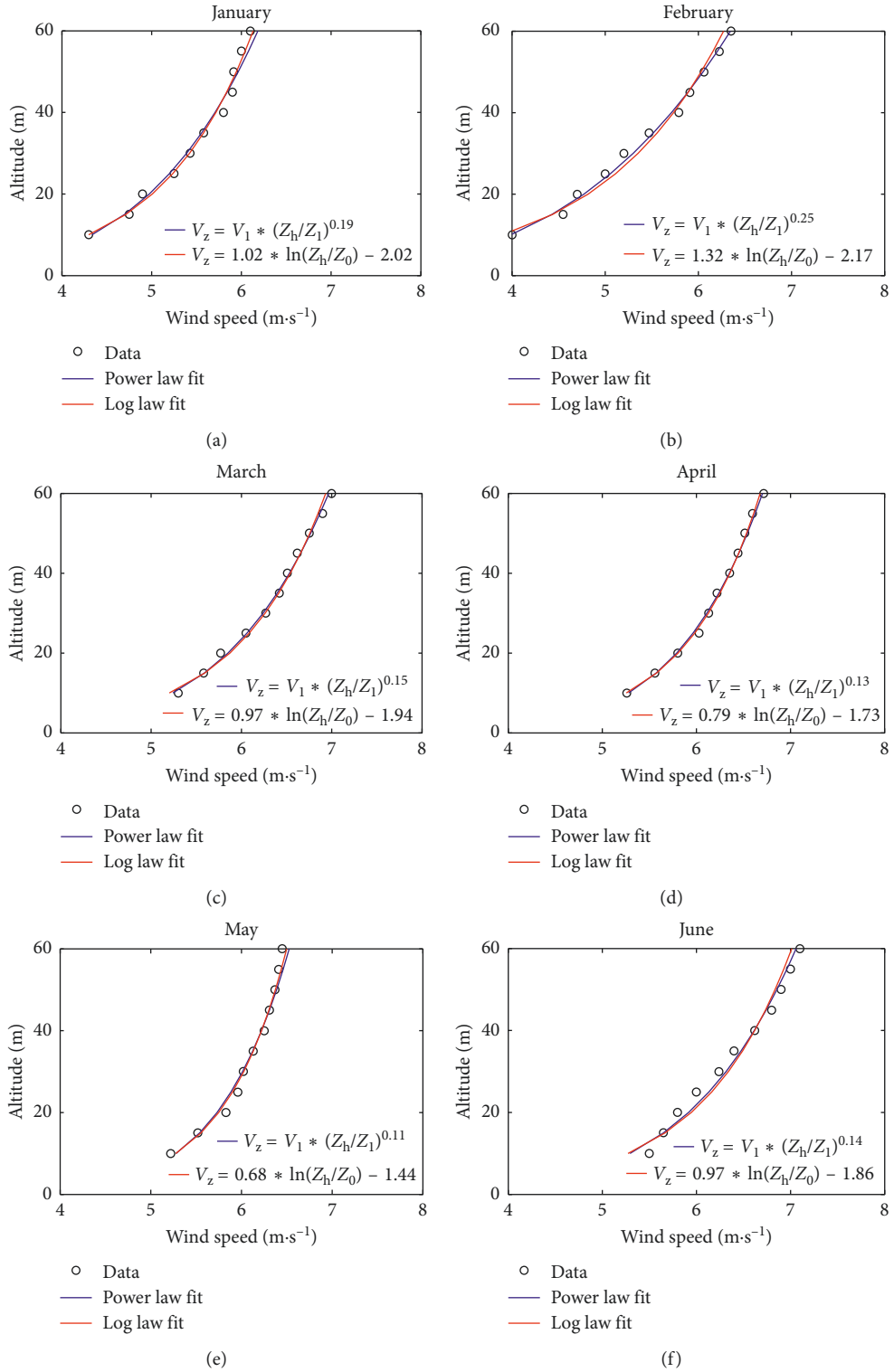

Figure 5: Continued.

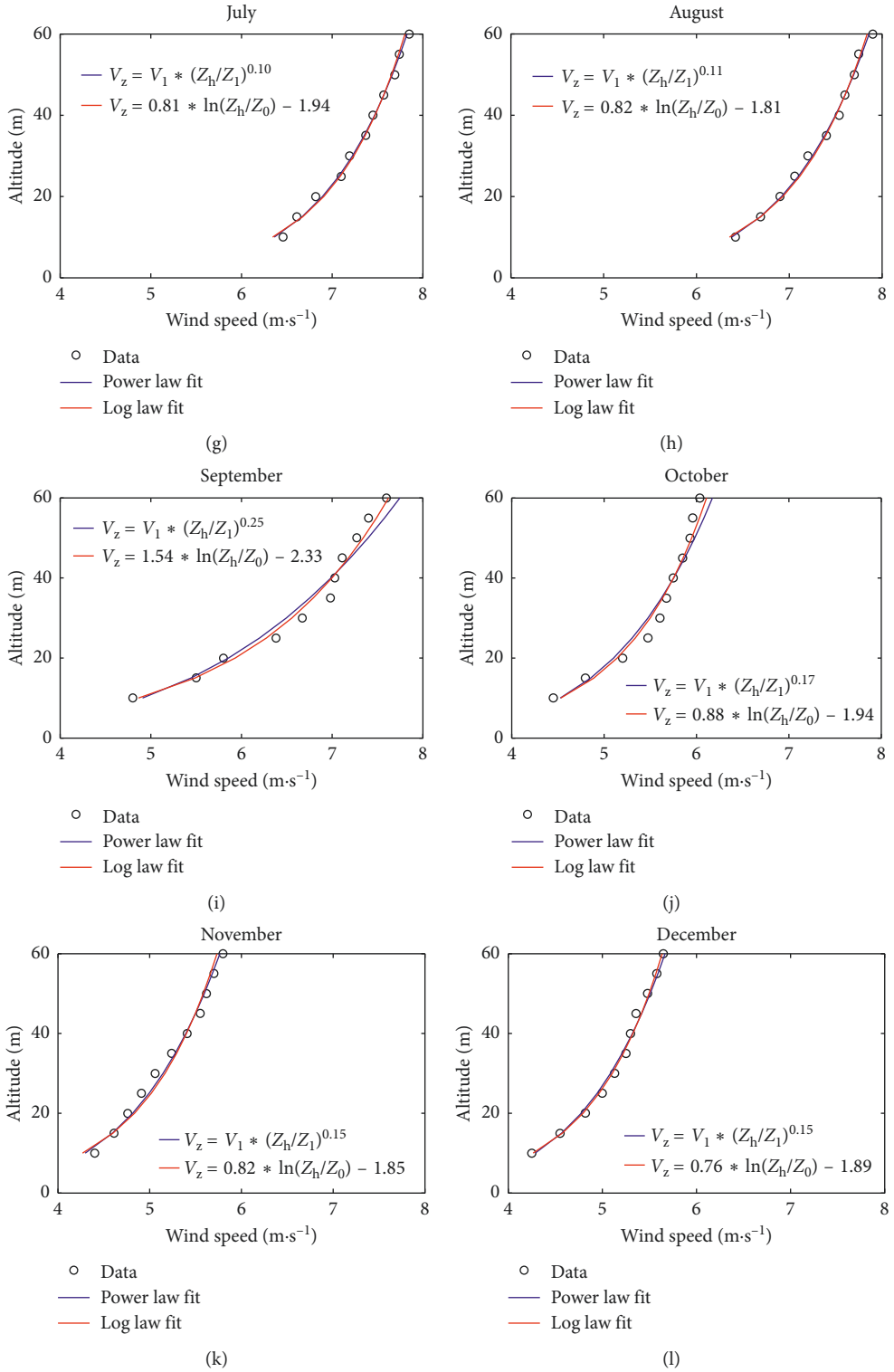

Figure 5: (a–l) Adjustments of the daily vertical profile of the wind speed at monthly scale from January to December (2013–2016).

Table 2: Adjustment parameters of the log-linear law and power law models on Cotonou site.

	Jan	Feb	Mar	Apr	May	Jun	Jul	Aug	Sep	Oct	Nov	Dec
A	1.02	1.32	0.96	0.79	0.68	0.97	0.81	0.83	1.54	0.88	0.82	0.76
B	1.94	0.85	2.98	3.43	3.70	3.04	4.47	4.44	1.32	2.5	2.38	2.5
α	0.19	0.25	0.15	0.13	0.11	0.14	0.10	0.11	0.25	0.17	0.15	0.15

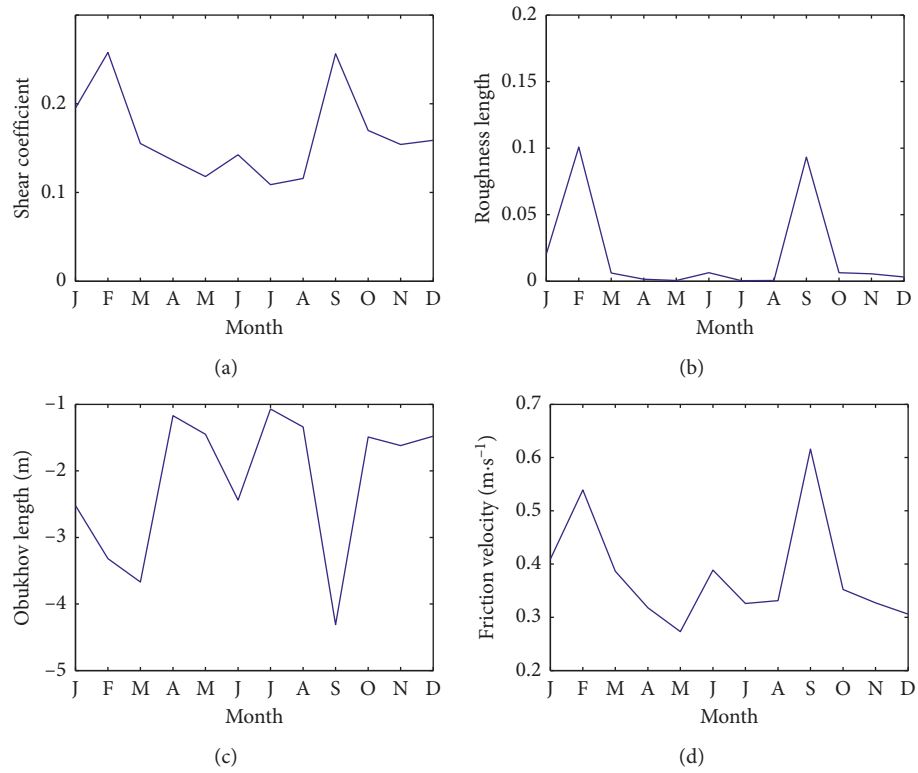

Figure 6: The wind shear average parameters. (a) Average shear coefficient. (b) Average roughness length. (c) Average Obukhov length. (d) Average friction velocity (2013–2016).

Table 3: Root-Mean-Squared Error (RMSE) and Mean Absolute Error (MAE) values for different law fits corresponding to the 10–60 m extrapolation range (2013–2016).

	Power law		Log law	
	RMSE (m·s^{-1})	MAE (m·s^{-1})	RMSE (m·s^{-1})	MAE (m·s^{-1})
January	0.06	0.06	0.05	0.04
February	0.07	0.05	0.10	0.09
March	0.04	0.03	0.05	0.04
April	0.03	0.02	0.02	0.01
May	0.05	0.04	0.04	0.03
June	0.09	0.07	0.11	0.09
July	0.04	0.03	0.05	0.04
August	0.03	0.02	0.04	0.03
September	0.14	0.13	0.10	0.08
October	0.10	0.07	0.07	0.06
November	0.06	0.05	0.07	0.06
December	0.04	0.03	0.03	0.02

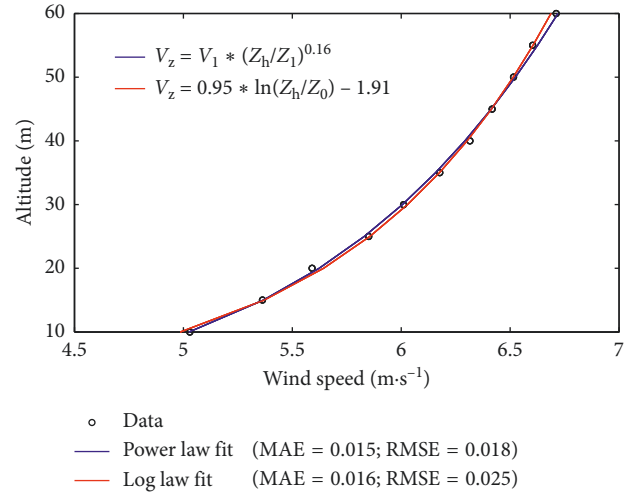

Figure 7: Adjustment of the daily vertical profile of the wind speed at annual scale (2013–2016).

strongly correlated. The correlation coefficients between wind shear coefficient and friction velocity, roughness and friction velocity, and wind shear coefficient and roughness are estimated, respectively, at 0.91, 0.94, and 0.93. The roughness is an increasing function of wind shear and ground friction velocity near the surface. During the months of February and September, the highest values of these three parameters are, respectively, estimated at 0.258; 0.10 m; 0.54 m·s^{-1} and 0.257; 0.09 m; 0.62 m·s^{-1}. In July, the lowest values of wind shear coefficient and average surface roughness length are, respectively, evaluated at 0.11; 3.7×10^{-4} m. The lowest value of friction velocity is observed in December and estimated at 0.30 m·s^{-1}. The annual average surface roughness length is 7×10^{-3} m. As for the friction velocity, the annual value is estimated at 0.38 m·s^{-1}. The low values observed for the roughness could be explained by changes in the characteristics of the ground surface at the site (grassland) compared to its cover (Figure 2). The wind direction also has a significant impact on this variability, particularly compared to the various obstacles encountered in the field (buildings or other

structures) and which would be the cause of the high values observed in February and September. Referring to the study of [54–57] reported by [58, 59], the value of the Hellman coefficient for similar sites to ours ranges between 0.09 and 0.20 for an unstable atmosphere. These values correspond to most of our results which indicate that the shear coefficient varies from 0.11 to 0.26 under the same atmospheric stability conditions. The discrepancies observed would be due to the presence of a few buildings on our study site which is not far from the airport. By exploiting the studies of [60], the value of the roughness length indicated for a coastal area is estimated at 5×10^{-3} m. This result is close to the one we found at our study site which was averagely estimated at 7×10^{-3} m. The findings concerning the friction velocity are quite close to those obtained by [61, 62] at the coastal sites and are, respectively, estimated at an average of $0.55\,\mathrm{m{\cdot}s^{-1}}$ and $0.43\,\mathrm{m{\cdot}s^{-1}}$.

According to the analysis of Figure 6(c), it follows that during the whole measurement period, the values obtained for the Obukhov length belong to the atmospheric stability class A based on the values taken from Table 1. The atmosphere is therefore unstable during this period. These results are corroborated by a large number of studies such as those of [21, 63] which indicate that the atmosphere is unstable during the day. As far as [64] are concerned, they assert that between 06:00 and 18:00 MST, the atmosphere is generally unstable with a few temperature inversions in the late afternoon. Earlier on, [65] believed already that an unstable stratification occurs when there is much surface warming and causes diurnal convective movements near the surface. Also, a seasonal variation of this parameter is observed. The lowest values recorded in January, February, March, and September, which are dry season periods in the study area [31], are, respectively, equal to −2.52 m, −3.32 m, −3.68 m, and −4.31 m. The highest values recorded in April, May, June, July, and October, which are rainy season periods [31], are, respectively, equal to −1.17 m, −1.45 m, −2.4 m, −1.07 m, and −1.5 m. These results then indicate that during the day and periods when the temperature is high on the ground such as the dry season, the atmosphere is more unstable due to the intense convection of air masses. This finding is consistent with the assertions of [21, 63–65]. However, in the months of August, November, and December, which are dry season periods, the values close to those obtained during the rainy season are recorded. They are estimated at −1.34 m, −1.62 m, and −1.48 m, respectively. This can be explained by the fact that August is the least warm month of the year due to the particular atmospheric circulation prevailing with the rise in the cold water level in the Atlantic Ocean [66]. There are thus fewer convective movements. On the other hand, during the months of November and December, the values obtained could be justified by the progressive arrival of harmattan in the study area which comes cooling the atmosphere. Figure 8 shows the average monthly variations in these parameters according to the years.

On Figure 8, we notice that the four parameters, namely, wind shear coefficient, roughness length, friction velocity, and length of Obukhov have a seasonal and interannual variability. Figure 8(a) shows the variation in the wind shear coefficient. It varies from 0.08 in July 2013 and May 2015 to 0.34 in February 2015. In Figure 8(b), the lowest values of the roughness length are recorded during the month of July and April 2013 as well as May 2015. The highest value, equal to 0.33 m, is obtained in February 2015. In Figure 8(c), the friction velocity at the ground level varies between $0.15\,\mathrm{m{\cdot}s^{-1}}$ obtained in April 2013 and $0.85\,\mathrm{m{\cdot}s^{-1}}$ in February 2015. In Figure 8(d), the variation in the Obukhov length is shown. We note that whatever the period of the year is, the atmosphere is unstable during the period of data measure. The values vary from −7.52 and −7.17, respectively, in June 2013 and June 2014 to −0.45 in October 2014.

In short, the month of February turned out to be the period when the shear coefficient, the roughness length, and the friction velocity reached their highest values. All these results, which are partly in agreement with those obtained in Figure 6, confirm the large variability of the wind. And so, for a better evaluation of the wind resource on a site, studies on wind parameters upon several years are therefore essential.

3.3. Comparative Study of Wind Extrapolation Models. Figures 9 and 10 show a comparison between some wind extrapolation models taken in the literature (and applied as is without previous calibration or best-fitting process), with the proposed model (best fitting equation) and the data. It should be noted that the wind shear parameters obtained on our site were used in these extrapolations models. The two best fitting equations obtained based on the two laws being almost identical in terms of performance on our site, for the comparative study, we used the best fitting equation based on the power law because it requires less adjustment parameters.

The MAE values between the empirical data and the available models are calculated and set out in Table 4.

The analysis of the results obtained shows that throughout the year, the proposed model (best fitting equation) gives the best adjustment of the wind vertical profile. The lowest MAE values for this model are obtained in Table 4. As for the other adjustment models, in general, they do not correspond to the measures. They underestimate or overestimate the empirical data according to the month which is considered. By considering the annual wind profile, all models available and exploited in this study underestimate the data as shown in Figure 10. However, it should be noted that during the months of February and November, the models of [12, 67] give, respectively, a good adjustment with the data. The errors estimation of MAE is equal to 0.08 and 0.07. Also the model of [13] obtained in Algeria gives also a good approximation of the wind profile for the months of May and August. The MAE values estimated for these months are, respectively, equal to 0.05 and 0.03.

In short, this comparative study indicates us that the models developed on a given site are not always adapted to other sites. This same observation has been made by [25–27] who, after testing the reliability of these empirical formulas,

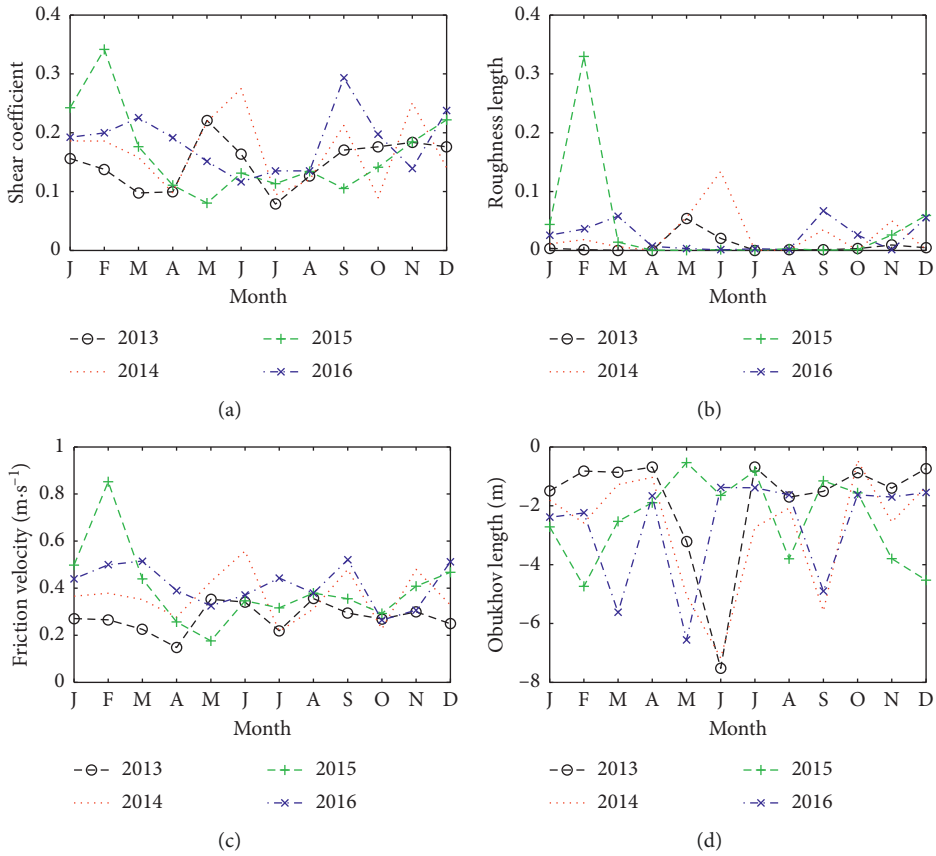

Figure 8: The wind shear average parameters following the year. (a) Shear coefficient. (b) Roughness length. (c) Friction velocity. (d) Obukhov length (2013–2016).

have reached inconclusive results. The establishment of an empirical model of the wind extrapolation for each site is therefore appropriate in order to reduce estimation errors, as proposed by [26].

3.4. Vertical Profile of the Wind Diurnal Cycle. Figure 11 shows the variation of Obukhov length during its diurnal and nocturnal cycle. Obukhov length is determined by equation (4).

Referring to Table 1, the analysis of the graphs in this figure therefore indicates that from 09:00 to 18:00 MST, the atmosphere is generally unstable. This result confirms the one obtained with radiosonde data at 10:30 MST and those of [63–65]. For the other periods of the day, it is stable. Based on these observations, the average vertical profile of the wind is presented during diurnal cycle between 09:00 and 18:00 MST in Figure 12. From the power law that requires less parameters (equations (14) and (17)) of wind shear and the wind data recorded at 10 m from the ground, we have determined this profile by extrapolation.

In Figure 12, the vertical profile of wind convective diurnal cycle generally confirms lots of the observations and analysis made from Figure 3. During this cycle, the windiest months are August, July, and March with average speeds evaluated, respectively, at 8.07 m·s^{-1}, 7.81 m·s^{-1}, and 7.13 m·s^{-1} at 60 m from the ground. The lowest values of wind speed are recorded in November, October, and December, respectively, for values of 4.98 m·s^{-1}, 5.14 m·s^{-1}, and 5.25 m·s^{-1} at 60 m. The wind shear coefficient is evaluated during this cycle at 0.20. These wind speed values are therefore database for the investors in the wind energy field for a first decision-making step in order to develop this source of renewable energy in our subregion.

4. Conclusions

In this study, the radiosonde data from the Cotonou airport site were used to evaluate different techniques for extrapolating wind speed. The power and logarithmic law models were therefore evaluated for the atmospheric instability class. The parameters of these models were estimated for the study site. These models were then compared with the models available in the bibliography. The most suitable model for the site was then used to extrapolate the vertical profile of wind convective diurnal cycle from the data measured at 10 m from the ground. The main results of our study are summarized as follows:

(i) The power and logarithmic laws give the best adjustments of the average annual wind speed. The error estimators RMSE and MAE are, respectively, evaluated at 0.018; 0.015 and 0.025; 0.016.

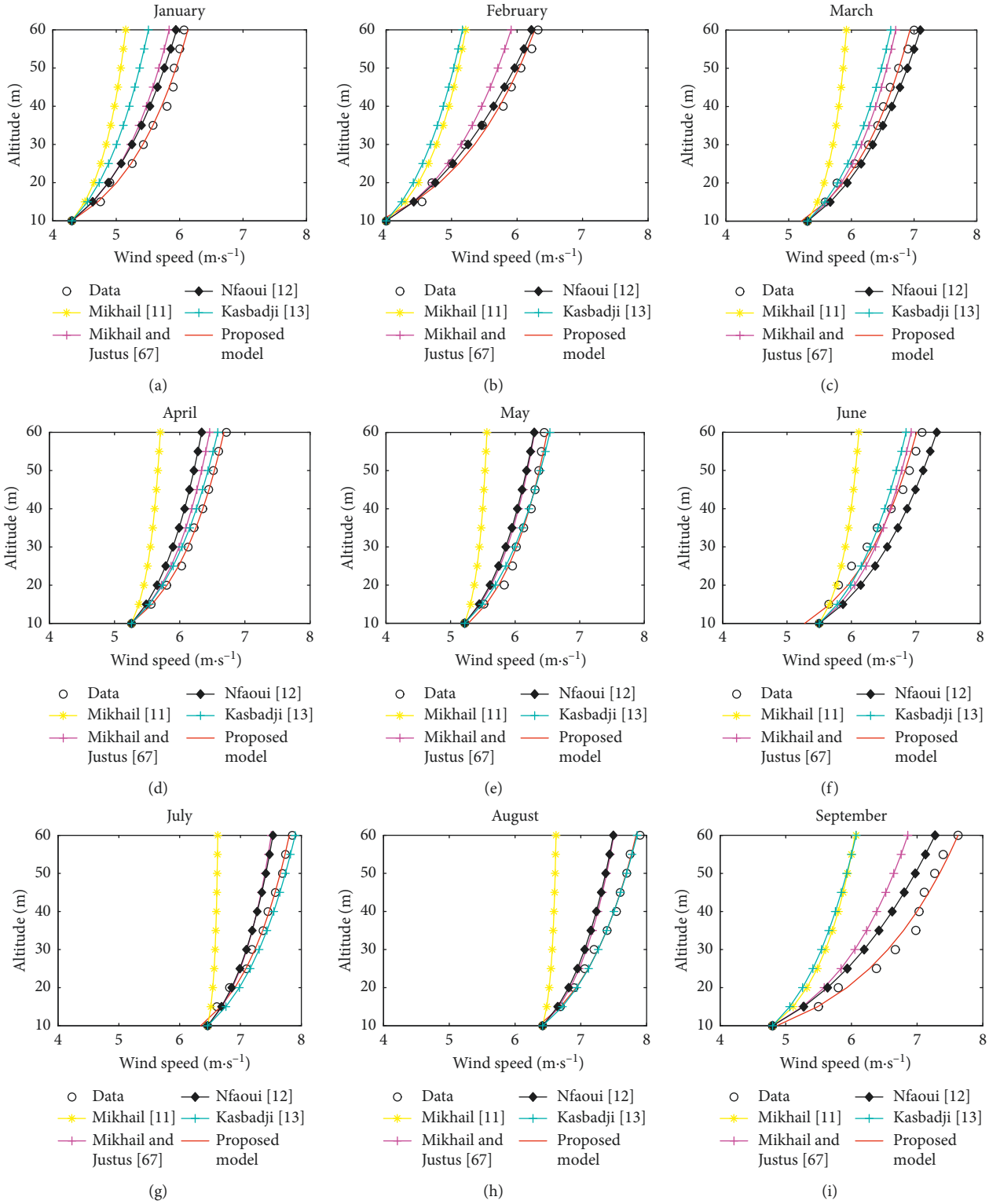

Figure 9: Continued.

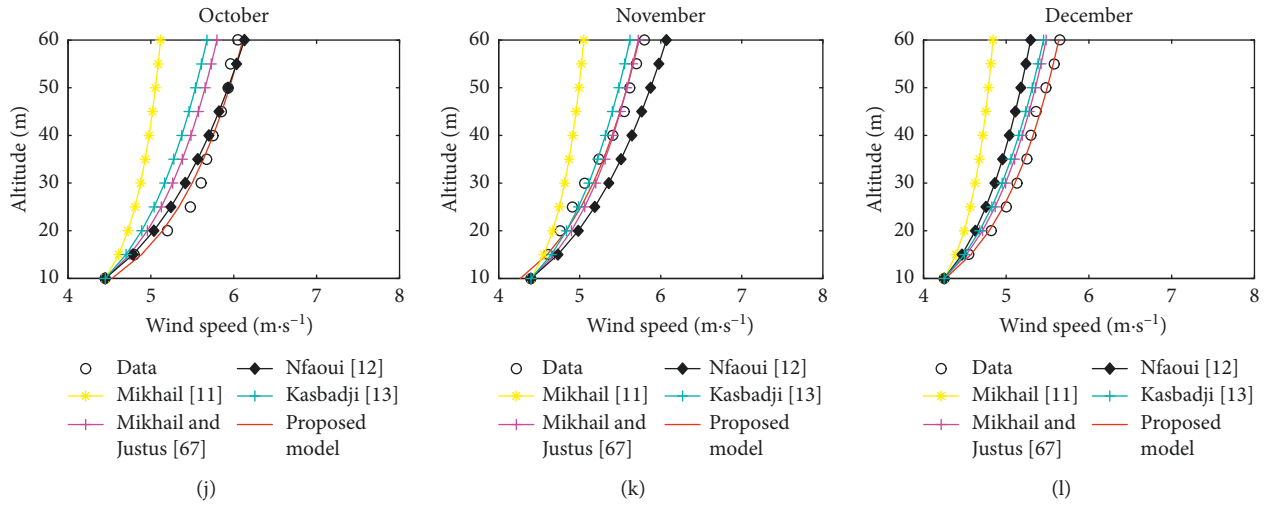

Figure 9: Monthly comparison of wind speed vertical extrapolation models (a–l) (2013–2016).

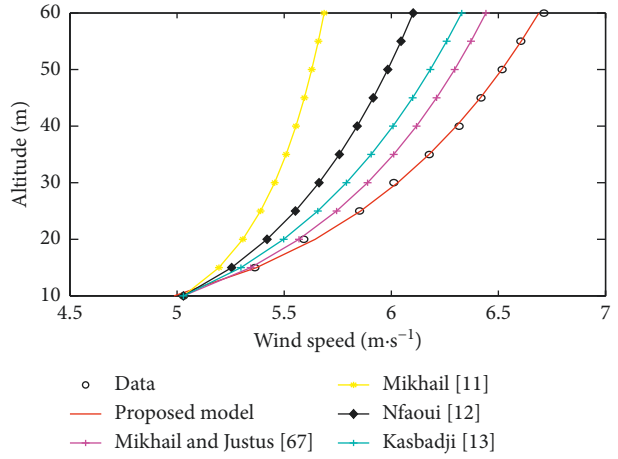

Figure 10: Annual comparison of wind speed vertical extrapolation models (2013–2016).

Table 4: Mean Absolute Error (MAE) between models and measure corresponding to the 10–60 m extrapolation range (2013–2016).

	Proposed model (best fitting equation) MAE (m·s^{-1})	Mikhail and Justus [67] MAE (m·s^{-1})	Mikhail [11] MAE (m·s^{-1})	Nfaoui et al. [12] MAE (m·s^{-1})	Kasbadji [13] MAE (m·s^{-1})
Jan	0.06	0.19	0.60	0.15	0.41
Feb	0.05	0.21	0.59	0.08	0.66
Mar	0.03	0.13	0.58	0.10	0.18
Apr	0.02	0.14	0.59	0.23	0.08
May	0.04	0.15	0.59	0.17	0.05
Jun	0.07	0.13	0.46	0.24	0.14
Jul	0.03	0.17	0.68	0.16	0.08
Aug	0.02	0.19	0.72	0.21	0.03
Sep	0.13	0.51	0.99	0.32	1.01
Oct	0.07	0.23	0.64	0.08	0.32
Nov	0.05	0.072	0.37	0.22	0.08
Dec	0.03	0.11	0.50	0.24	0.14
Yearly	0.018	0.14	0.6	0.37	0.23

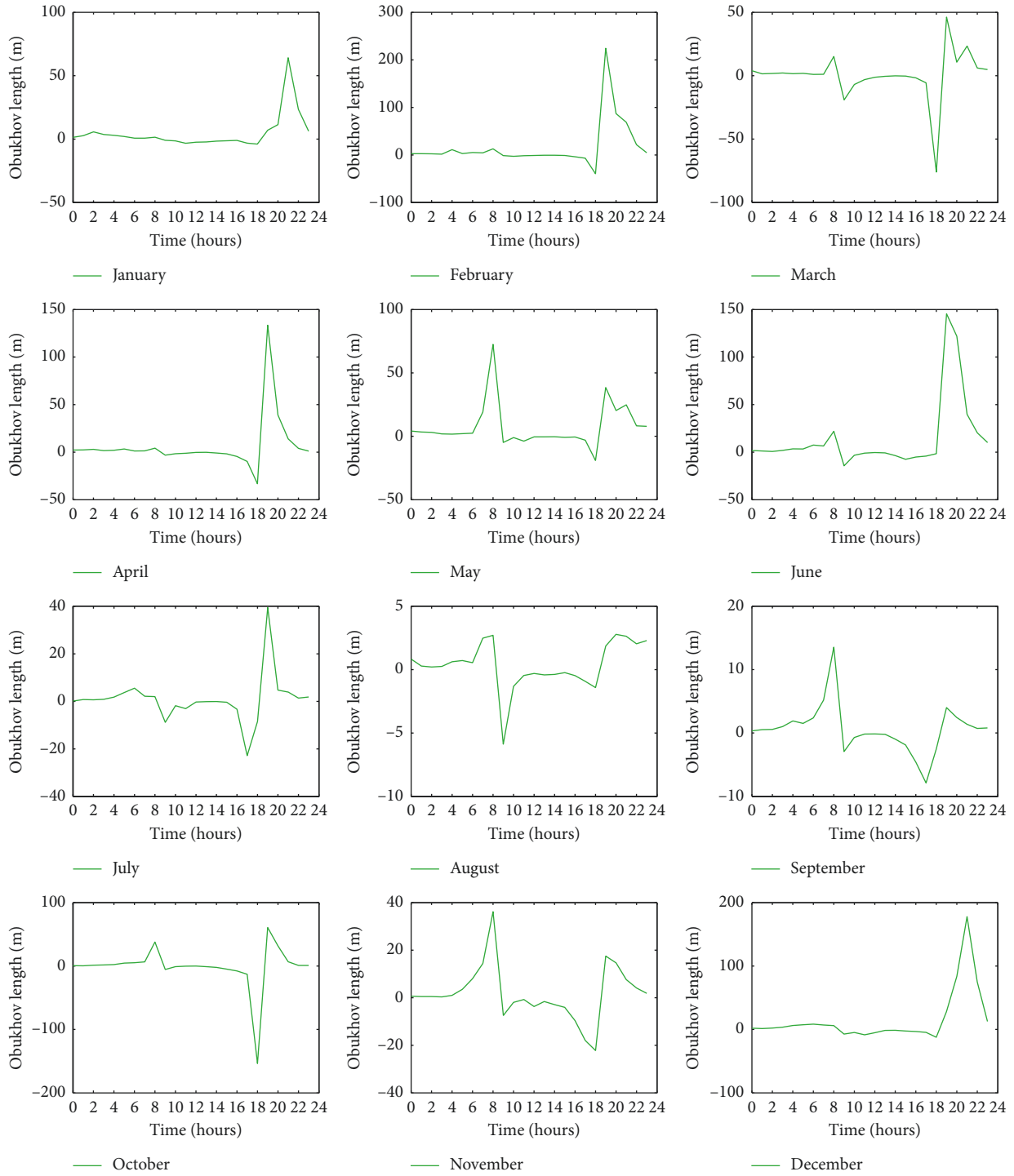

Figure 11: Diurnal and nocturnal cycle variation in the Obukhov length for a typical day on a monthly time scale (2013–2016).

(ii) At the site, the atmosphere is generally unstable from 09:00 to 18:00 MST and stable during other periods of the day. The annual average wind shear coefficient during the convective diurnal cycle is estimated at 0.20, the surface roughness length at 7×10^{-3} m, and the friction velocity is 0.38 m·s^{-1}.

(iii) The comparative study between the extrapolation models of wind and the data reveals that throughout the year, only the proposed model (best fitting equation) always agrees with the data. The lowest RMSE and MAE values are obtained for this model unlike others models. These empirical formulas encountered in the bibliography and

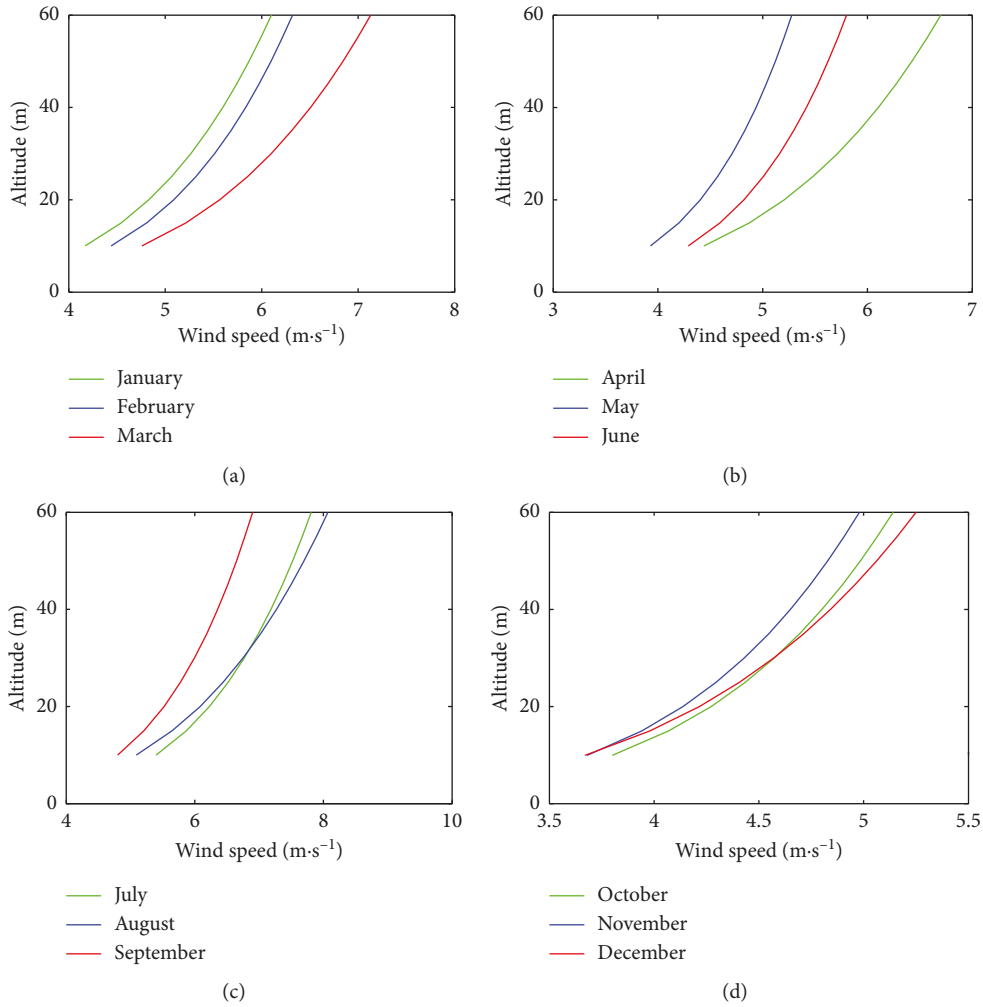

Figure 12: Average vertical profile of wind convective diurnal cycle at monthly scale. (a) January to March, (b) April to June, (c) July to September, and (d) October to December (2013–2016).

established in given meteorological conditions (favourable for the use of Monin–Obukhov theory) and for particular sites display limits over another similar sites. Therefore, we propose the establishment of a specific model for each site considered.

(iv) Finally, the vertical profile of the wind during the diurnal cycle (09:00 to 18:00 MST) was determined from the extrapolation of the wind speeds measured at 10 m by the power law which requires fewer parameters than the logarithmic law. The average wind speed is estimated at 8.07 m·s^{-1} for the windiest month (August) and 4.98 m·s^{-1} for the least windy month (November) 60 m from the ground.

These results are therefore useful to investors in the wind energy field in order to exploit suitably this energy source in our subregion. In the future, the performance of the power and logarithmic laws adjustment will be examined for the other atmospheric stability conditions, in particular stable conditions that generally occur during the nocturnal cycle.

Data Availability

The radiosondage/wind at 10 m/ambient temperature data used to support the findings of this study were supplied by Agency for Air Navigation Safety in Africa and Madagascar (ASECNA/Benin Representation) under license and so cannot be made freely available. Requests for access to these data should be made to ASECNA/Benin Representation, BP 96 and 08-179, Cotonou, phone: (229) 21 30 01 61/48 21 30 14 13/02 92; fax: (229) 21 30 08 39.

Conflicts of Interest

The authors declare that they have no conflicts of interest.

Authors' Contributions

The study was completed with cooperation between all authors.

Acknowledgments

The authors of this paper sincerely thank the Agency for Air Navigation Safety in Africa and Madagascar (ASECNA) for having made the radiosonde sounding data available to them, data which were used to carry out this research work.

References

[1] L. Morales, F. Lang, and C. Mattar, "Mesoscale wind speed simulation using CALMET model and reanalysis information: an application to wind potential," *Renewable Energy*, vol. 48, pp. 57–71, 2012.

[2] X. Li and H. Wang, "Stochastic time series reconstruction of future wind farm output," in *Proceedings of IEEE Innovative Smart Grid Technologies Asia*, Tianjin, China, May 2012.

[3] G. Grassi and P. Vecchio, "Wind energy prediction using a two-hidden layer neural network," *Communications in Nonlinear Science and Numerical Simulation*, vol. 15, no. 9, pp. 2262–2266, 2010.

[4] Y.-L. Tu, T.-J. Chang, C.-L. Chen, and Y.-J. Chang, "Estimation of monthly wind power outputs of WECS with limited record period using artificial neural networks," *Energy Conversion and Management*, vol. 59, pp. 114–121, 2012.

[5] G. Gualtieri and S. Secci, "Extrapolating wind speed time series vs. Weibull distribution to assess wind resource to the turbine hub height: a case study on coastal location in Southern Italy," *Renewable Energy*, vol. 62, pp. 164–176, 2014.

[6] A. S. Monin and A. M. Obukhov, "Basic laws of turbulent mixing in the ground layer of the atmosphere," *Proceedings of Geophysics Institute, National Academy of Science*, vol. 151, pp. 163–187, 1954.

[7] G. P. van den Berg, "Wind turbine power and sound in relation to atmospheric stability," *Wind Energy*, vol. 11, no. 2, pp. 151–169, 2008.

[8] S. Drechsel, G. J. Mayr, J. W. Messner, and R. Stauffer, "Wind speeds at heights crucial for wind energy: measurements and verification of forecasts," *Journal of Applied Meteorology and Climatology*, vol. 51, no. 9, pp. 1602–1617, 2012.

[9] E. Hau, *Wind Turbines: Fundamentals, Technologies, Application, Economics*, Springer, Berlin, Germany, 2013.

[10] C. G. Justus and A. Mikhail, "Height variation of wind speed and wind distributions statistics," *Geophysical Research Letters*, vol. 3, no. 5, pp. 261–264, 1976.

[11] A. S. Mikhail, "Height extrapolation of wind data," *Journal of Solar Energy Engineering*, vol. 107, no. 1, pp. 10–14, 1985.

[12] H. Nfaoui, B. J. Bahraoui, and A. A. M. Sayigh, "Wind characteristics and wind energy potential in Morocco," *Solar Energy*, vol. 63, no. 1, pp. 51–60, 1998.

[13] N. M. Kasbadji, "Evaluation du gisement énergétique éolien–contribution à la détermination du profil vertical de la vitesse du vent," Thèse de Doctorat, Université Abou BekrBelkaïd de Tlemcen, Tlemcen, Algérie, 2006.

[14] S. Rehman and N. M. Al-Abbadi, "Wind shear coefficient, turbulence intensity and wind power potential assessment for Dhulom, Saudi Arabia," *Renewable Energy*, vol. 33, no. 12, pp. 2653–2660, 2008.

[15] A. M. Omer, "On the wind energy resources of Sudan," *Renewable and Sustainable Energy Reviews*, vol. 12, no. 8, pp. 2117–2139, 2008.

[16] M. A. Lackner, A. L. Rogers, J. F. Manwell, and J. G. McGowan, "A new method for improved hub height mean wind speed estimates using short-term hub height data," *Renewable Energy*, vol. 35, no. 10, pp. 2340–2347, 2010.

[17] A. Oluleye and S. B. Ogungbenro, "Estimating the wind energy potential over the coastal stations of Nigeria using power law and diabatic methods," *African Journal of Environmental Science and Technology*, vol. 5, no. 11, pp. 985–992, 2011.

[18] G. Gualtieri and S. Secci, "Comparing methods to calculate atmospheric stability-dependent wind speed profiles: a case study on coastal location," *Renewable Energy*, vol. 36, no. 8, pp. 2189–2204, 2011b.

[19] A. Peña, S.-E. Gryning, and C. B. Hasager, "Measurements and modelling of the wind speed profile in the marine atmospheric boundary layer," *Boundary-Layer Meteorology*, vol. 129, no. 3, pp. 479–495, 2008.

[20] J. F. Newman and P. M. Klein, "The impacts of atmospheric stability on the accuracy of wind speed extrapolation methods," *Resources*, vol. 3, no. 1, pp. 81–105, 2014.

[21] G. Gualtieri, "Atmospheric stability varying wind shear coefficients to improve wind resource extrapolation: a temporal analysis," *Renewable Energy*, vol. 87, pp. 376–390, 2016.

[22] M. E. Okorie, F. Inambao, and Z. Chiguvare, "Evaluation of wind shear coefficients, surface roughness and energy yields over inland locations in Namibia," *Procedia Manufacturing*, vol. 7, pp. 630–638, 2017.

[23] A. Tenneekes, "The logarithmic wind profile," *Journal of the Atmospheric Sciences*, vol. 30, no. 2, pp. 234–238, 1973.

[24] M. Schwartz and D. Elliott, "Towards a wind energy climatology at advanced turbine hub-heights," in *Proceedings of 15th Conference on Applied Climatology*, Savannah, GA, USA, May 2005.

[25] E. W. Peterson and J. P. Hennessey, "On the use of power laws for estimates of wind power potential," *Journal of Applied Meteorology*, vol. 17, no. 3, pp. 390–394, 1978.

[26] D. Poje and B. Cividini, "Assessment of wind energy potential in Croatia," *Solar Energy*, vol. 41, no. 6, pp. 543–554, 1988.

[27] S. Doutreloup, X. Fettweis, J. Beaumet, and M. Erpicum, "Comparaison entre le profil vertical de la vitesse du vent observé dans les basses couches de la troposphère et celui simulé par le modèle WRF en Belgique," in *Proceedings of XXVIIe Colloque de l'Association Internationale de Climatologie*, Dijon, France, July 2014.

[28] C. N. Awanou, J. M. Degbey, and E. Ahlonsou, "Estimation of the mean wind energy available in Benin (Ex Dahomey)," *Renewable Energy*, vol. 1, no. 5-6, pp. 845–853, 1991.

[29] M. A. Houekpoheha, B. Kounouhewa, B. N. Tokpohozin, and C. N. Awanou, "Estimation de la puissance énergétique éolienne à partir de la distribution de weibull sur la côte Béninoise de Cotonou dans le Golfe de Guinée," *Revue des Energies Renouvelables*, vol. 17, pp. 489–495, 2014.

[30] A. B. Akpo, J. C. T. Damada, H. E. V. Donnou, B. Kounouhewa, and C. N. Awanou, "Estimation de la production énergétique d'un aérogénérateur sur un site isolé dans la région côtière du Bénin," *Revue des Energies Renouvelables*, vol. 18, no. 3, pp. 457–468, 2015.

[31] C. S. U. Y. Allé, A. A. Afouda, K. E. Agbossou, and H. Guibert, "Évolution des descripteurs intrasaisonniers des saisons pluvieuses au sud-Bénin entre 1951 et 2010," *American Journal of Scientific Research*, no. 94, pp. 55–68, 2013, ISSN 2301-2005.

[32] E. Fiogbe, A. Dossou-Yovo, and E. Ogouwale, *Rapport National sur l'Environnement Marin et Côtier du Bénin*,

Direction Générale de l'Environnement, CEDA, Benin, 2007.
[33] H. M. Konow, *Tall wind profiles in heterogeneous terrain*, Ph.D. thesis, University of Hamburg, Hamburg, Germany, 2015.
[34] E.-M. Giannakopoulou and R. Nhili, "WRF model methodology for offshore wind energy applications," *Advances in Meteorology*, vol. 2014, Article ID 319819, 14 pages, 2014.
[35] S. M. Boudia, "Optimisation de l'évaluation temporelle du gisement énergétique éolien par simulation numérique et contribution à la réactualisation de l'atlas des vents en Algérie," Thèse de Doctorat, Université de Tlemcen Abou-Bakr Blekaïd, Tlemcen, Algeria, 2012.
[36] C. A. Paulson, "The mathematical representation of wind speed and temperature profiles in the unstable atmospheric surface layer," *Journal of Applied Meteorology*, vol. 9, no. 6, pp. 857–861, 1970.
[37] J. A. Businger, J. C. Wyngaard, Y. Izumi, and E. F. Bradley, "Flux-profile relationships in the atmospheric surface layer," *Journal of the Atmospheric Sciences*, vol. 28, no. 2, pp. 181–189, 1971.
[38] R. Weber, "Estimators for the standard deviations of lateral, longitudinal and vertical wind components," *Atmospheric Environment*, vol. 32, no. 21, pp. 3639–3646, 1998.
[39] B. Lange, S. Larsen, J. Hojstrup, and R. Barthelmie, "Modelling the vertical wind speed and turbulence intensity profiles at prospective offshore wind farm sites," in *Proceedings of 2002 Global Windpower Conference*, Paris, France, 2002.
[40] A. A. Grachev and C. W. Fairall, "Dependence of the Monin-Obukhov stability parameter on the bulk Richardson number over the ocean," *Journal of Applied Meteorology*, vol. 36, no. 4, pp. 406–414, 1997.
[41] N. Sucevic and Z. Djurisic, "Vertical wind speed profiles estimation recognizing atmospheric stability," in *Proceedings of EEEIC 2011 Conference Proceedings*, Rome, Italy, May 2011.
[42] F. Bañuelos-Ruedas, C. Angeles-Camacho, and S. Rios-Marcuello, "Analysis and validation of the methodology used in the extrapolation of wind speed data at different heights," *Renewable and Sustainable Energy Reviews*, vol. 14, no. 8, pp. 2383–2391, 2010.
[43] G. Hellman, "Uber die bewegung der luft in den untersten schichten der atmosphere," *Meteorologische Zeitschrift*, vol. 34, pp. 273–285, 1916.
[44] D. A. Spera and T. R. Richards, "Modified power law equations for vertical wind profiles," in *Proceedings of Conference and Workshop on Wind Energy Characteristics and Wind Energy Siting*, Portland, OR, USA, June 1979.
[45] G. Gualtieri and S. Secci, "Wind shear coefficients, roughness, length and energy yield over coastal locations in Southern Italy," *Renewable Energy*, vol. 36, no. 3, pp. 1081–1094, 2011a.
[46] S. Kulkarni and H.-P. Huang, "Changes in surface wind speed over North America from CMIP5 model projections and implications for wind energy," *Advances in Meteorology*, vol. 2014, Article ID 292768, 10 pages, 2014.
[47] N. M. Zoumakis, "Dependence of the wind profile power law exponent on the Pasquill stability classes and height interval in a stably stratified surface boundary layer," *Il Nuovo Cimento C*, vol. 16, no. 1, pp. 79–81, 1993.
[48] S. Akpinar and E. K. Akpinar, "Wind energy analysis based on maximum entropy principle (MEP)-type distribution function," *Energy Conversion and Management*, vol. 48, no. 4, pp. 1140–1149, 2007.
[49] F. Ben Amar, M. Elamouri, and R. Dhifaoui, "Energy assessment of the first wind farm section of Sidi Daoud, Tunisia," *Renewable Energy*, vol. 33, no. 10, pp. 2311–2321, 2008.
[50] T. Chai and R. R. Draxler, "Root mean square error (RMSE) or mean absolute error (MAE)?–arguments against avoiding RMSE in the literature," *Geoscientific Model Development*, vol. 7, no. 3, pp. 1247–1250, 2014.
[51] L. Le Barbé, T. Lebel, and D. Tapsoba, "Rainfall variability in West Africa during the years 1950–90," *Journal of Climate*, vol. 15, no. 2, pp. 187–202, 2002.
[52] M. R. Elkinton, A. L. Rogers, and J. G. McGowan, "An investigation of wind-shear models and experimental data trends for different terrains," *Wind Engineering*, vol. 30, no. 4, pp. 341–350, 2006.
[53] D. Khalfa, A. Benretem, L. Herous, and I. Meghlaoui, "Evaluation of the adequacy of the wind speed extrapolation laws for two different roughness meteorological sites," *American Journal of Applied Sciences*, vol. 11, no. 4, pp. 570–583, 2014.
[54] A. D. Busse and J. R. Zimmerman, *Users Guide for the Climatological Dispersion Model*, Environmental Protection Agency, Washington, DC, USA, 1973.
[55] J. S. Touma, "Dependence of the wind profile power law on stability for various locations," *Journal of the Air Pollution Control Association*, vol. 27, no. 9, pp. 863–866, 1977.
[56] TA-Luft, Erste Allgemeine Verwaltungsvorschrift zum Bundes-Immissionsschutzgesetz-Technische Anleitung zur Reinhaltung der Luft (First general directive to the federal immission protection act-Technical guideline for clean air), 1986, in German.
[57] D. Kühner, "Excess attenuation due to meteorological influences and ground impedance," *Acustica-Acta Acustica*, vol. 84, no. 5, pp. 870–883, 1998.
[58] M. M. Ichenial, A. El Hajjaji, and A. Khamlichi, "Effect of atmospheric stability on the estimation of wind power potential," in *Proceedings of MATEC Web of Conferences*, vol. 83, Melaka, Malaysia, April 2016.
[59] G. P. van den Berg, "Effects of the wind profile at night on wind turbine sound," *Journal of Sound and Vibration*, vol. 277, no. 4-5, pp. 955–970, 2004.
[60] Y. Chang, J. Tan, S. Grimmond, and Y. Tang, "Distribution of aerodynamic roughness based on land cover and DEM—a case study in shanghai, China," in *Proceedings of ICUC9—9th International Conference on Urban Climate Jointly with 12th Symposium on the Urban Environment*, Toulouse, France, July 2015.
[61] A. Peña and S.-E. Gryning, "Charnock's roughness length model and non-dimensional wind profiles over the sea," *Boundary-Layer Meteorology*, vol. 128, no. 2, pp. 191–203, 2008.
[62] D. Jarmalavičius, J. Satkūnas, G. Zilinskas, and D. Pupienis, "The influence of coastal morphology on wind dynamics," *Estonian Journal of Earth Sciences*, vol. 61, no. 2, pp. 120–130, 2012.
[63] S. Yahaya, J. P. Frangi, and D. C. Richard, "Turbulent characteristics of a semiarid atmospheric surface layer from cup anemometers—effects of soil tillage treatment (Northern Spain)," *Annales Geophysicae*, vol. 21, no. 10, pp. 2119–2131, 2003.
[64] B. K. Fritz, W. C. Hoffmann, Y. Lan, S. J. Thomson, and Y. Huan, "Low-level atmospheric temperature inversions and atmospheric stability: characteristics and impacts on agricultural applications," *Agricultural Engineering International: CIGR Journal Ejournal PM*, vol. 10, 2008.

[65] T. Burton, D. Sharpe, N. Jenkins, and E. Bossyanyi, *Wind Energy Handbook*, John Wiley & Sons, Hoboken, NJ, USA, 2001.

[66] M. Leduc-Leballeur, "Influence océanique du Golfe de Guinée sur la mousson en Afrique de l'ouest," Thèse de Doctorat, Université Pierre et Marie Curie Paris VI, Paris, France, 2012.

[67] A. S. Mikhail and C. G. Justus, "Comparison of height extrapolation models and sensitivity analysis," *Wind Engineering*, vol. 5, no. 2, pp. 10–14, 1981.